PHILIPS

Computed Tomography

Whitepaper

Detector-based spectral CT delivers on the promise of increased accuracy for proton therapy

Inaccuracy in proton stopping-power ratios (SPR) calculated from conventional HU-based CT images, and the associated proton beam range uncertainty, is a well-known limitation in realizing the full potential of proton therapy. This error has been documented in literature to be approximately 3%. Multi-energy CT has shown promise in reducing SPR inaccuracy and proton range uncertainty. This white paper analyzes peer-reviewed publications that document the accuracy of electron density (ED) and effective atomic number (Z-effective) images from various multi-energy technologies. It then compares the resulting SPR accuracy from these different inputs. The analysis shows a range of quantitative accuracy in the ED and Z-effective images across multi-energy CT technologies, and the resulting SPR values, with dual-layer detector-based spectral CT providing the most accurate results. This analysis demonstrates a spectral SPR uncertainty of less than 1% for detector-based spectral CT.

Over the past decade, the use of proton therapy has been increasing rapidly. The sharp dose cutoff of the proton Bragg peak allows for sharper dose delivery potential than would be possible in external beam photon therapy.[1,2] As a result, surrounding organs at risk can be more effectively spared, decreasing potential side effects. Alternatively, it enables dose escalation, if necessary.

Locating the proton Bragg peak in the body requires an estimation of the proton stopping-power of tissues. Historically, conventional CT Hounsfield units (HU) are translated to proton stopping-power ratios (SPR) through stoichiometric calibration curves. However, this HU-based SPR assessment is associated with an uncertainty of 3%, which translates to an uncertainty of 3 mm for a target region at 10 cm depth.[3] With this, the precision of proton energy deposition is not fully exploited, detracting from the overall potential of proton therapy.

In contrast to conventional HU-based indirect SPR calculations, novel CT techniques can allow for a direct SPR calculation.[3–10] These techniques can be categorized as source-based dual-energy CT (DECT) or detector-based spectral CT. The second category consists of dual-layer CT (DLCT) and photon-counting CT (PCCT), employing energy-integrating or photon-counting detectors, respectively. To calculate SPR with the aforementioned multi-energy CT techniques, two datasets are needed: Electron density (ED) and effective atomic number (Z_{eff}). Subsequently, SPR is directly calculated from a formula like the Bethe-Bloch equation. To minimize SPR errors, ED and Z_{eff} values must be highly accurate and quantitative.[11]

Recent studies have shown that the accuracy and precision of ED and Z_{eff} depend on the technique used.[12–14] For the source-based DECT techniques (i.e. spin-spin, kVp-switching, split-filter, or dual-source), acquisition of spectral data has to be predefined. The reason for this is the inherent compromise, such as a reduced gantry rotation time, limited reconstruction field-of-view, increased radiation dose, or reduced temporal resolution. On the other hand, for detector-based spectral CT techniques (i.e. DLCT and PCCT), presetting is not required as every scan provides spectral data (in addition to true conventional images).

For DLCT, direct SPR calculation is possible with the use of the Philips MultiModality Simulation Workspace (MM SIM*) software package. For this, ED and Z_{eff} maps can be sent automatically from the CT console to MM SIM*. Here, SPR can be directly calculated using the Bethe Bloch equation based on three different methods (Figure 1).[15–17] Also, the SPR can be calculated for carbon (270.55 MeV), low energy protons (117 MeV) and high energy protons (200 MeV) (Figure 2).

While recent studies have described ED and Z_{eff} accuracies, an analysis on the link of these accuracies with SPR accuracy is lacking. We have, therefore, performed a literature search to identify the accuracies of ED and Z_{eff} on commercially available DECT and spectral CT systems for non-gated scans, to assess how these accuracies translate into SPR uncertainties.

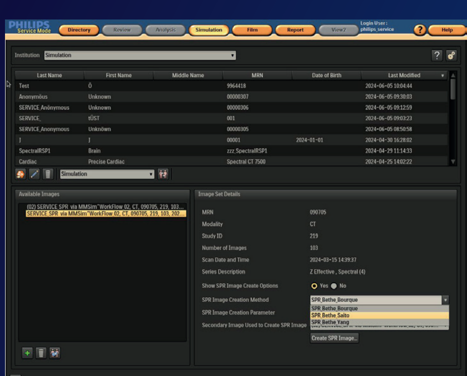

Figure 1 MM SIM*, showing SPR methods

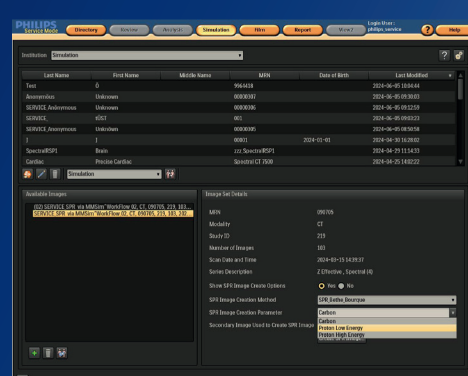

Figure 2 MM SIM*, showing SPR parameters

*Not available in all geographies

Inaccuracy in proton stopping-power ratios (SPR) calculated from conventional HU-based CT images, and the associated proton beam range uncertainty, is a well-known limitation in realizing the full potential of proton therapy. This error has been documented in literature to be approximately 3%. Multi-energy CT has shown promise in reducing SPR inaccuracy and proton range uncertainty.

Key points

- Analyzes peer-reviewed publications that document the accuracy of electron density (ED) and effective atomic number (Z-effective) images from various multi-energy technologies.
- Compares the resulting SPR accuracy from these different inputs.
- The analysis shows a range of quantitative accuracy in the ED and Z-effective images across multi-energy CT technologies, and the resulting SPR values, with dual-layer detector-based spectral CT providing the most accurate results.
- Analysis demonstrates a spectral SPR uncertainty of less than 1% for detector-based spectral CT, which has been further confirmed in published literature.

Utilization of spectral CT is expected to increase for dose calculation in proton therapy because it can reduce this uncertainty to less than 1%.[18]

Methods

We have performed a literature search on Pubmed, using the following search query on June 11th 2024: ((photon counting) OR (dual energy)) + ((electron density) or (effective atomic number)) + (phantom).

We have included only peer-reviewed journal articles written in English that describe accuracy measurements of Z-effective and electron density (excluding non-commercial implementations) using the Gammex electron density CT Phantoms 467 (Gammex-RMI, Middleton, WI, USA).

We extracted the reported ED and Z_{eff} accuracies from the tables or figures in the articles and reported them in this white paper. Furthermore, we have used these ED and Z_{eff} accuracies to calculate the uncertainties that these inaccuracies imply on SPR values calculated with the Bethe-Bloch equation, using the polynomial fit proposed by Bourque (see appendix).[19]

Results

The Embase search resulted in 154 peer-reviewed journal articles. Out of these, four papers met our inclusion requirements, describing measurements on various DE and spectral CT solutions. One paper reported SPR uncertainty on photon counting CT, but because these results were not based on Z_{eff} and ED maps, this article was excluded.[20] Another paper used an incorrect Z_{eff} exponent for the calculation of the reference materials (3.3 and not the system assumed value of 2.94).[21] Therefore, this article was also excluded. An overview of the included papers can be found in Table 1.

The reported ED and Z_{eff} accuracies based on non-gated CT scans, and the calculated implied SPR accuracies are shown in Table 2, Table 3, and Table 4, respectively. One article did not report ED results and therefore we were not able to calculate the implied SPR uncertainties.

The average absolute reported differences for Z_{eff} ranged from 1.6% (dual-layer) to 10.6% (split-filter) and for ED from 0.4% (dual-layer) to 3.2% (split-filter). The average absolute SPR uncertainties implied by these Z_{eff} and ED uncertainties ranged from 0.3% (dual-layer) to 5.0% (split-filter) (Table 5). Importantly, the maximum SPR uncertainty exceeded 2% for all techniques, apart from the dual-layer solution for which the maximum SPR uncertainty was found to be 0.9%.

Article	Year	Types of multi-energy CT tested	Reported
Goodsitt, et al.[2]	2011	KV-switching DECT (KV-DECT)	Z-effective
Almeida, et al.[3]	2017	Dual-Source DECT (DS-DECT) and Split-filter DECT (SF-DECT)	Z-effective, electron density
Hua, et al.[4]	2018	Spectral-detector CT (spectral CT)	Z-effective, electron density

Table 1 Overview of articles included in the literature review analysis

Discussion

The results reported in Table 5 demonstrate that there is a large variation in the accuracy of ED and Z_{eff}, between tube-based and detector-based spectral CT solutions. As a result, the implied SPR accuracies varied considerably between the solutions.

One article has reported on the accuracy of dual-layer spectral CT.[14] In this study, Hua et al. compensated for the limited thickness (5 cm) of the Gammex 467 phantom. A reduced pitch and collimation were used to compensate for the assumptions on the body composition of the system's scatter correction algorithms.[14] These adjusted scan settings are not needed in clinical scanning, because normal patient dimensions will fulfill the scatter assumptions.

For PCCT, direct SPR calculation is not possible in clinical practice as both Z_{eff} and ED maps cannot be generated on the currently available system. However, Hu et al.[20] reported on the SPR uncertainty while using virtual monoenergetic images (VMI) for an indirect SPR calculation. On the same phantom (Gammex 467), the VMI-based SPR uncertainty was found to be 1.27% for this PCCT.

From this literature study, we can conclude that Hua, et al.[14] were able to report the highest Z_{eff} and ED accuracies. For this, the authors used a dual-layer spectral CT, which showed an implied SPR uncertainty of 0.3%, which is the most optimal implied SPR error in this review.

An SPR uncertainty of 0.3% is in line with both Faller, et al.[22] and Longarino, et al.[23] who (using the Gammex 467 Phantom) also reported SPR uncertainties below 1% on the Philips IQon Spectral CT and Spectral CT 7500 (the latest generation detector-based spectral CT from Philips), respectively. The difference is that the calculated value in the current evaluation is a theoretical value, while the SPR uncertainties of Faller et al. (0.6%) and Longarino et al. (0.7%) are end-to-end measurements.

In conclusion, the detector-based spectral CT showed the lowest average absolute differences for both Z_{eff} and ED, which subsequently results in the lowest SPR uncertainty.

The detector-based spectral CT reproducibly delivers on the promise to provide SPR with an uncertainty below 1%, which results in the highest clinically available SPR accuracy.[18]

Clinical relevance

To precisely estimate the Bragg peak location, exact estimations of the stopping power of tissues are crucial. Historically, the proton stopping-power has been calculated through a stoichiometric lookup table that converts conventional HU directly into SPR values. This technique is associated with range uncertainties of around 3%, meaning that if the target is 10 cm in the body, the position of the Bragg peak has a location uncertainty of 3 mm in the direction of the beam.

The promise of spectral CT for proton therapy planning is an increase in SPR accuracy. Philips MMSIM offers functionality that can take ED and Z_{eff} results and generate SPR maps according to the Bethe-Bloch equation. However, any error in these ED and Z_{eff} measurements will directly translate into SPR uncertainties. It is therefore crucial that the quantitative accuracy of the spectral measurements is assured.

In this paper we provide an overview of the reported ED and Z_{eff} measured on the Gammex 467. It demonstrates that the accuracy of ED and Z_{eff} results in some DECT implementations are not sufficient to ensure errors under 1%. In some systems the average error even exceeds 3%, meaning that a conventional stoichiometric lookup table would yield better accuracy.

The review shows that detector-based spectral CT reproducibly assures both average and maximum SPR uncertainties under 1%. This conclusion was in line with a recent study by Longarino, et al.[23], that reported an average SPR uncertainty of 0.7% on the Gammex Phantom model 467 on Spectral CT 7500, which uses the latest generation spectral-detector system from Philips.

Gammex 467 insert	Dual-source (Siemens Flash)	Dual-source (Siemens Force)	Split-filter (Siemens Edge)	Dual-layer (Philips IQon)	kVp-switching (GE Discovery CT750 HD)
Lung (LN-300)	-4.2%	-5.3%	-20.4%	7.0%	0.0%
Liver	0.0%	-1.0%	-1.7%	0.7%	-1.1%
Bone (CB2 - 50% mineral)	0.7%	-0.3%	1.4%	-0.2%	-3.9%
Bone (B-200)	0.8%	1.7%	4.2%	0.2%	-3.5%
Cortical bone	-0.2%	0.3%	0.3%	-0.3%	-3.6%
Lung (LN-450)	-7.0%	-2.3%	-14.7%	5.8%	0.0%
Brain	-6.8%	-5.3%	-28.3%	1.2%	15.1%
Adipose	-4.9%	-3.6%	-22.3%	1.6%	-0.6%
Inner bone	-0.3%	1.3%	0.0%	0.0%	-3.4%
Bone (CB2 - 30% mineral)	-0.5%	-1.9%	-5.6%	0.0%	-3.4%
True water	3.1%	0.7%	-11.6%	-2.3%	5.5%
Breast	1.9%	-2.5%	-16.3%	0.2%	3.6%

Table 2 Percentage errors in the effective atomic number (ΔZ_{eff}) measured on dual-source and split-filter DECT as described by Almeida, et al.[24], on Dual-layer spectral CT as described by Hua et al.[14], and on kVp-switching DECT as described by Goodsitt, et al.[12]

Gammex 467 insert	Dual-source (Siemens Flash)	Dual-source (Siemens Force)	Split-filter (Siemens Edge)	Dual-layer (Philips IQon)	kVp-switching (GE Discovery CT750 HD)
Lung (LN-300)	0.4%	1.2%	15.3%	0.8%	n/a
Liver	-0.4%	-0.1%	0.7%	0.6%	n/a
Bone (CB2 - 50% mineral)	-0.5%	0.0%	-0.3%	0.5%	n/a
Bone (B-200)	-0.3%	-0.3%	-0.8%	0.1%	n/a
Cortical bone	0.2%	0.0%	-0.5%	-0.1%	n/a
Lung (LN-450)	1.0%	0.2%	7.2%	0.5%	n/a
Brain	1.3%	1.0%	3.1%	1.1%	n/a
Adipose	0.7%	0.5%	2.4%	0.0%	n/a
Inner bone	0.4%	-0.4%	0.6%	0.1%	n/a
Bone (CB2 - 30% mineral)	0.3%	0.5%	2.1%	0.1%	n/a
True water	0.6%	0.6%	3.2%	0.1%	n/a
Breast	0.3%	0.0%	2.1%	0.0%	n/a

Table 3 Percentage errors in electron density (Δ ED) measured on dual-source and split-filter DECT as described by Almeida, et al.[24], on detector-based spectral CT as described by Hua et al.[14], and on kVp-switching DECT as described by Goodsitt, et al.[12]

Gammex 467 insert	Dual-source (Siemens Flash)	Dual-source (Siemens Force)	Split-filter (Siemens Edge)	Dual-layer (Philips IQon)	kVp-switching (GE Discovery CT750 HD)
Lung (LN-300)	0.7%	1.6%	18.5%	-2.1%	n/a
Liver	-0.4%	0.0%	0.8%	1.3%	n/a
Bone (CB2 - 50% mineral)	-0.6%	0.1%	-0.6%	0.3%	n/a
Bone (B-200)	-0.4%	-0.5%	-1.1%	0.1%	n/a
Cortical bone	0.2%	-0.1%	-0.6%	0.0%	n/a
Lung (LN-450)	1.6%	0.4%	9.0%	-2.4%	n/a
Brain	2.5%	2.0%	9.4%	-2.1%	n/a
Adipose	1.6%	1.2%	7.1%	0.2%	n/a
Inner bone	0.4%	-0.5%	0.6%	0.1%	n/a
Bone (CB2 - 30% mineral)	0.3%	0.7%	2.6%	0.0%	n/a
True water	0.4%	0.6%	4.5%	-0.4%	n/a
Breast	0.5%	0.3%	4.9%	-0.1%	n/a

Table 4 Implied percentage errors in stopping-power ratio (Δ SPR) based on effective atomic number and electron density data for dual-source and split-filter DECT as described by Almeida, et al.[24], on detector-based spectral CT as described by Hua et al[14], and on kVp-switching DECT as described by Goodsitt, et al.[12] For kVp-switching, Δ SPR could not be calculated, due to missing ED information in the described paper.

CT technique category	CT system	Stopping-power ratio uncertainty		
		Minimum	Maximum	Absolute mean
Source-based	**Dual-source** (Siemens Flash)	-0.6%	2.5%	0.8%
	Dual-source (Siemens Force)	-0.5%	2.0%	0.7%
	Split-filter (Siemens Edge)	-1.1%	18.5%	5.0%
	kVp-switching (GE Discovery CT750 HD)	n/a	n/a	n/a
Detector-based	**Dual-layer** (Philips Spectral CT)	-0.3%	0.9%	0.3%

Table 5 Implied percentage errors in sstopping-power ratio (Δ SPR) over all Gammex 467 inserts (minimum, maximum, and absolute mean values) based on effective atomic number and electron density data for dual-source and split-filter DECT as described by Almeida, et al.24, on detector-based spectral CT as described by Hua et al.[14], and on kVp-switching DECT as described by Goodsitt, et al.[12] For kVp-switching, Δ SPR could not be calculated, due to missing ED information in the described paper.

References

1. Bragg WH, Kleeman R. LXXIV. On the ionization curves of radium. The London, Edinburgh, and Dublin Philosophical Magazine and Journal of Science. 1904;8(48):726-738. doi:10.1080/14786440409463246
2. Durante M, Orecchia R, Loeffler JS. Charged-particle therapy in cancer: clinical uses and future perspectives. Nat Rev Clin Oncol. 2017;14(8):483-495. doi:10.1038/nrclinonc.2017.30
3. Bär E, Lalonde A, Royle G, Lu HM, Bouchard H. The potential of dual-energy CT to reduce proton beam range uncertainties. Med Phys. 2017;44(6):2332-2344. doi:10.1002/mp.12215
4. Yang M, Virshup G, Clayton J, Zhu XR, Mohan R, Dong L. Theoretical variance analysis of single- and dual-energy computed tomography methods for calculating proton stopping power ratios of biological tissues. Phys Med Biol. 2010;55(5):1343-1362. doi:10.1088/0031-9155/55/5/006
5. Hudobivnik N, Schwarz F, Johnson T, et al. Comparison of proton therapy treatment planning for head tumors with a pencil beam algorithm on dual and single energy CT images. Med Phys. 2016;43(1):495-504. doi:10.1118/1.4939106
6. Zhu J, Penfold SN. Dosimetric comparison of stopping power calibration with dual-energy CT and single-energy CT in proton therapy treatment planning. Med Phys. 2016;43(6Part1):2845-2854. doi:10.1118/1.4948683
7. Bär E, Lalonde A, Zhang R, et al. Experimental validation of two dual-energy CT methods for proton therapy using heterogeneous tissue samples. Med Phys. 2018;45(1):48-59. doi:10.1002/mp.12666
8. Möhler C, Russ T, Wohlfahrt P, et al. Experimental verification of stopping-power prediction from single- and dual-energy computed tomography in biological tissues. Phys Med Biol. 2018;63(2):025001. doi:10.1088/1361-6560/aaa1c9
9. Wohlfahrt P, Möhler C, Richter C, Greilich S. Evaluation of Stopping-Power Prediction by Dual- and Single-Energy Computed Tomography in an Anthropomorphic Ground-Truth Phantom. International Journal of Radiation Oncology*Biology*Physics. 2018;100(1):244-253. doi:10.1016/j.ijrobp.2017.09.025
10. Xie Y, Ainsley C, Yin L, et al. Ex vivo validation of a stoichiometric dual energy CT proton stopping power ratio calibration. Phys Med Biol. 2018;63(5):055016. doi:10.1088/1361-6560/aaae91
11. Paganetti H. Range uncertainties in proton therapy and the role of Monte Carlo simulations. Phys Med Biol. 2012;57(11):R99-R117. doi:10.1088/0031-9155/57/11/R99
12. Goodsitt MM, Christodoulou EG, Larson SC. Accuracies of the synthesized monochromatic CT numbers and effective atomic numbers obtained with a rapid kVp switching dual energy CT scanner. Med Phys. 2011;38(4):2222-2232. doi:10.1118/1.3567509
13. Almeida IP, Schyns LEJR, Ollers MC. Dual-energy CT quantitative imaging : a comparison study between twin-beam and dual-source CT scanners. Published online 2017:171-179.
14. Hua C, Shapira N, Merchant TE, Klahr P, Yagil Y. Accuracy of electron density, effective atomic number, and iodine concentration determination with a dual-layer dual-energy computed tomography system. Med Phys. 2018;45(6):2486-2497. doi:10.1002/mp.12903
15. Saito M, Sagara S. Simplified derivation of stopping power ratio in the human body from dual-energy <scp>CT</scp> data. Med Phys. 2017;44(8):4179-4187. doi:10.1002/mp.12386
16. Yang M, Virshup G, Clayton J, Zhu XR, Mohan R, Dong L. Theoretical variance analysis of single- and dual-energy computed tomography methods for calculating proton stopping power ratios of biological tissues. Phys Med Biol. 2010;55(5):1343-1362. doi:10.1088/0031-9155/55/5/006
17. Bourque AE, Carrier JF, Bouchard H. A stoichiometric calibration method for dual energy computed tomography. Phys Med Biol. 2014;59(8):2059-2088. doi:10.1088/0031-9155/59/8/2059
18. Kruis MF. Improving radiation physics, tumor visualisation, and treatment quantification in radiotherapy with spectral or dual-energy CT. J Appl Clin Med Phys. 2022;23(1). doi:10.1002/acm2.13468
19. Bourque AE, Carrier JF, Bouchard H. A stoichiometric calibration method for dual energy computed tomography. Phys Med Biol. 2014;59(8):2059-2088. doi:10.1088/0031-9155/59/8/2059
20. Hu G, Niepel K, Risch F, et al. Assessment of quantitative information for radiation therapy at a first-generation clinical photon-counting computed tomography scanner. Front Oncol. 2022;12. doi:10.3389/fonc.2022.970299
21. Ohira S, Washio H, Yagi M, et al. Estimation of electron density, effective atomic number and stopping power ratio using dual-layer computed tomography for radiotherapy treatment planning. Physica Medica. 2018;56:34-40. doi:10.1016/j.ejmp.2018.11.008
22. Faller FK, Mein S, Ackermann B, Debus J, Stiller W, Mairani A. Pre-clinical evaluation of dual-layer spectral computed tomography-based stopping power prediction for particle therapy planning at the Heidelberg Ion Beam Therapy Center. Phys Med Biol. 2020;65(9):095007. doi:10.1088/1361-6560/ab735e
23. Longarino FK, Kowalewski A, Tessonnier T, et al. Potential of a Second-Generation Dual-Layer Spectral CT for Dose Calculation in Particle Therapy Treatment Planning. Front Oncol. 2022;12. doi:10.3389/fonc.2022.853495
24. Almeida IP, Schyns LEJR, Öllers MC, et al. Dual-energy CT quantitative imaging: a comparison study between twin-beam and dual-source CT scanners. Med Phys. 2017;44(1):171-179. doi:10.1002/mp.12000

Appendix

$$\mathrm{SPR} = \frac{\rho_e}{\rho_{e,w}} \bullet \frac{\ln\left(\frac{2m_e c^2 \beta^2}{I_m (1-\beta^{2})}\right) - \beta^2}{\ln\left(\frac{2m_e c^2 \beta^2}{I_w (1-\beta^{2})}\right) - \beta^2}$$

As stated in the introduction, SPR for a medium relative to water is approximated following the Bethe equation:
with ρ_e and $\rho_{e,w}$ the electron densities of the medium (input from the spectral reconstruction) and water respectively.
Other parameters are:

- β is the velocity of the particle beam relative to the speed of light c (dependent on the energy of the proton beam):

$$\beta^2 = 1 - \frac{1}{\left(1 + \frac{E}{m_p c^2}\right)^2}$$

- $m_e c^2$ the electron mass (511 keV)
- $m_p c^2$ the proton mass (938 MeV)
- E is the proton beam kinetic energy. In this evaluation a relatively low energy of 117.0 MeV is used.
- I_m is the mean excitation energy of the medium (computed with the effective atomic number from the spectral reconstruction)
- I_w the mean excitation energy of water (78.73 eV).

$$I_m = \begin{cases} a_{1,1}Z + a_{1,0} & Z < 6.26 \\ a_{2,5}Z^5 + a_{2,4}Z^4 + a_{2,3}Z^3 + a_{2,2}Z^2 + a_{2,1}Z + a_{2,0} & 6.26 \leq Z \leq 13.52 \\ a_{3,1}Z + a_{3,0} & 13.52 < Z \end{cases}$$

To compute the excitation energy of the medium based on the effective atomic, the polynomial fit proposed by Bourque is used[7]:
In these equations, Z is the effective atomic number. The values of the constants are: $a_{1,1}$=14.007762, $a_{1,0}$=-24.414214, $a_{2,5}$=-0.005342, $a_{2,4}$=0.207079, $a_{2,3}$=-2.589844, $a_{2,2}$=8.339473, $a_{2,1}$=51.895887, $a_{2,0}$=-219.722173, $a_{3,1}$=11.794847, $a_{3,0}$=-47.707141.

The error in the stopping power is computed based on the errors in the electron density ρ_e and effective atomic number Z provided:

$$\mathrm{SPR}_{error} = \frac{\mathrm{SPR}\left(\rho_e (1 + \rho_{e,error}), Z\,(1 + Z_{error})\right) - \mathrm{SPR}(\rho_e Z)}{\mathrm{SPR}(\rho_e Z)}$$

4522 991 87291 * DEC 2024

How to reach us
Please visit www.philips.com